The Effect of Centrifugal Force on the Assembly and Crystallization of Binary Colloidal Systems: Towards Structural Gradients

Mengdi Chen[a,b], Helmut Cölfen[b] and Sebastian Polarz[b]

[a] School of Materials Science and Engineering, Northwestern Polytechnical University, 710072 Xi'an, P. R. China

[b] Department of Chemistry, University of Konstanz, Universitätsstr. 10, 78457 Konstanz, Germany

Reprint requests to Prof. Dr. S. Polarz and Prof. Dr. H. Cölfen.
E-mail: sebastian.polarz@uni-konstanz.de, helmut.coelfen@uni-konstanz.de

Z. Naturforsch. **2013**, *68b*, 103 – 110 / DOI: 10.5560/ZNB.2013-3001
Received January 4, 2013

In this study, the effect of centrifugal force on the assembly and crystallization of binary colloidal mixtures is demonstrated. Monolithic pieces have been prepared which are characterized by a structural gradient along the direction of the centrifugal force. For a given number ratio of monodisperse 154 and 300 nm latex spheres, the absolute latex concentration was varied and with it the sedimentation velocity of the individual particle species. For three different concentrations it has been demonstrated that the structure of the binary colloidal assembly obtained after centrifugation is affected significantly. For the largest initial latex absolute concentrations, the structural variation along the packed latex column in the ultracentrifuge tube is minimal, while a decrease in the absolute concentrations leads to crystalline packing in defined regions of the column. The observation of the thermodynamically favored structure resembling NaCl, but also of the aluminum boride AlB_2 analog as well as unordered, glass-like packing depending on the mutual latex concentration under unchanged particle number and size ratio, shows that by centrifugation kinetically favored states can be realized. This result implies that centrifugation of binary latex mixtures is a promising route for investigating the self-organization of binary colloidal systems since the sedimentation velocities of the two particle species are different, and thus the local concentrations and mixing ratios vary continuously also enabling rare packing motifs.

Key words: Binary Colloidal Crystal, Ultracentrifugation, Structural Gradient, Self Organization

Introduction

The world of crystals formed of atoms has been explored for more than one century. One way to look at such crystals is to imagine the packing of atoms as hard spheres. The number and complexity of potential structures increases strongly with the number of different constituents. Even for binary phases numerous possibilities exist. According to a very simple model the smaller element should fit as well as possible into the voids of the packing of the larger element. This together with other factors like coordination preference or particle charge determines the structure of the thermodynamically most stable phase. While for ionic crystals the numerical proportion of the two spheres (atoms) is fixed due to charge balance, for intermetallic phases a whole range of different compositions can be probed correlating to an enormous variety of structures. Furthermore, it is well known that the very same compound can also exist in energetically less favorable modifications, so-called polymorphs [1]. However, the "disadvantages" of the model of atoms as spheres are that they are extremely small, that not every sphere size (or ratio of two sphere sizes) is available, and that the interaction cannot be adjusted for two given sphere sizes.

Some of the mentioned problems can be addressed by the use of colloidal objects as supramolecular atoms. The crystallization of colloidal systems containing particles with monodisperse size distribution is already a quite mature topic [2 – 5]. First of all there exist powerful methods for the preparation of monodis-

perse, spherical particles with adjustable size [5, 6]. Monodisperse silica nanoparticles in the size regime from ≈ 50 nm to microns can be produced by variations of the so-called Stoeber process [7 – 11]. Much more recently reliable methods for the preparation of other inorganic colloids like metal nanoparticles or metal oxides with very narrow size distribution could be developed [12]. It is the advantage of the latter particles, seen from the perspective as superatoms, that their use can lead to novel properties like superparamagnetism and special plasmonic or catalytic activities [13]. Last but not least, emulsion polymerization is a powerful technique for obtaining macroscopic amounts of spherical, polymeric particles [14 – 17]. The polydispersity should be below 4 % to achieve a significant driving force for crystallization [18, 19]. A colloidal crystal is an ordered array of colloid particles, analogous to a standard crystal whose repeating subunits are atoms or molecules [19]. Common methods for obtaining colloidal crystals are centrifugation [20, 21], electrophoresis [22 – 24], and evaporation methods [2, 3, 25, 26]. The special interest in colloidal crystals lies mainly in their special optical properties [27, 28]. Because the periodicity of such colloidal crystals can be adjusted to be of the order of the wavelength of visible light, special features like a photonic band structure and ultimately photonic band gaps result, respectively forbidden zones for particular light wavelengths in the crystal [29].

The preparation of colloidal crystals containing two or even more sphere sizes is a much more difficult task. Some of the most important current achievements are mentioned here. However, the interested reader is also pointed towards the excellent review articles by Möhwald *et al.* in 2004 and by Stein *et al.* in 2011 [30, 31]. First work on binary colloidal crystals has focused on spherical, charge-stabilized particles [32 – 35]. Typically a face-centered cubic (fcc) structure of the larger spheres with different numbers of smaller spheres in octahedral or tetrahedral voids could be achieved [36]. A very successful method for the preparation of binary systems was presented in 2004 by Wang *et al.* [37, 38]. This method involves the layer-by-layer deposition of different silica or polymer beads [37, 38]. The observed packing was highly dependent on the chosen size ratio of the spherical colloids. The latter systems often involve equally charged particles. There is a slight electrostatic repulsion which has to be overcome by the crystallization force. However, one further advantage of using colloidal building blocks is that the charge can be adjusted *via* surface modification [39]. Then, it becomes possible to use colloids with opposite charges for mimicking ionic crystals [40], and in addition, entropic factors become much more important [41 – 43]. The success in the preparation of nano-sized, inorganic particles with extremely narrow size distribution was an important step because the range of the interaction potentials becomes large in relation to particle size [44 – 46]. In addition, the deviation from spherical size opens new vistas in colloidal crystallization [47]. Colloidal crystals with non-spherical crystalline nanosized building units in crystallographic register are called mesocrystals [48 – 51]. They are found to be of rapidly increasing importance, but their formation mechanisms are yet poorly understood [52 – 54]. A number of interesting binary structures of the NaCl, CsCl, NiAs, Cu_3Au, $MgZn_2$ type and others could be fabricated from nearly spherical building units [55 – 58].

While centrifugation is a good method to prepare colloidal crystals from monodisperse particle dispersions, it has not been explored for inducing the directed assembly of binary or even more complex mixtures.

It is important to note that not all the structures which have been predicted by theoretical methods could be verified experimentally [59 – 62]. Thus, it is a tempting goal to design an experiment in which all possible, structural configurations can be obtained simultaneously. Due to different sedimentation velocities of differently sized latexes, it should be possible to build up two different overlaid radial concentration gradients, scanning through a large variety of different combinations of particle sizes and concentrations in a single experiment. This is the idea, which we investigate in the present paper.

Experimental Section

Synthesis of polystyrene nanoparticles

Monodisperse, negatively charged polystyrene spheres were synthesized by emulsion polymerization using a jacketed cylindrical reaction vessel, connected to a reflux condenser and a glass stirrer powered by a mechanical device [17]. The vessel also contained a temperature sensor and an Ar/reagent inlet. The temperature was maintained through the jacket with the use of a circulating temperature bath. Styrene was distilled prior to use. Sodium styrene sulfonate, sodium persulfate, sodium sulfite and sodium hydrogen carbonate were used as received. The resulting disper-

sion was passed through filter paper and purified by exhaustive dialysis with a 15000-MW cut off (MWCO). Dialysis was carried out in a 1 L beaker of water which was changed daily until its electrical conductivity remained constant. The determination of the solid content of the dispersion was performed by gravimetry.

Fabrication of colloidal crystals

Polystyrene colloidal crystals were synthesized with the L-70 ultracentrifuge (Beckman instruments) using the Beckman SW 55 Ti Ultracentrifuge Rotor to maintain latex sedimentation as undisturbed as possible using 5 mL ULTRA CLEAR tubes. In this work a centrifugal speed of 5000 rpm was used if not stated otherwise. Centrifugal time was set empirically to the time when clear separation of sediment and solvent became visible in the centrifuge tube. For the binary systems, reference samples consisting only of 300 nm latex were used, and the centrifugal time was set to the time when all larger spheres just sedimented to the bottom of the centrifuge tube. After the desired centrifugation time had elapsed, the run was stopped and the solvent at the top part of the centrifuge tube was gently removed by filter paper. Then the centrifuge tube was placed in a desiccator over silica gel and slowly dried at room temperature. Typical drying took 5 d.

Characterization

Dynamic light scattering was carried out using a Zetasizer μV instrument (Malvern). Transmission electron microscopy (TEM) measurements were performed on a Zeiss Libra 120 apparatus. Analytical ultracentrifugation (AUC) sedimentation velocity experiments of polystyrene latexes were carried out on a Beckman Optima XL-I analytical ultracentrifuge (Beckman Coulter, Palo Alto, CA) equipped with absorbance and interference optics. The concentration of the sample for the determination of the particle size distribution was 10^{-4} g mL^{-1}. A UV/Vis multi-wavelength analytical ultracentrifuge [63, 64] developed as an open source instrument [65] was also used to determine the particle size distribution. UV/Vis optical spectra were obtained on a Varian Carey 100 spectrometer (Varian). To examine the structure of the binary latex mixtures, the dried sample was cut along the long axis of the sample column using a razor blade, and the direction along the centrifugal force was subsequently investigated by using a Zeiss 249 CrossBeam 1540XB scanning electron microscope.

Results and Discussion

Negatively charged, colloidal dispersions of polystyrene lattices (PS) were prepared by the method described in the Experimental Section [17]. The size of the PS spheres was characterized using dynamic light scattering (DLS), analytical ultracentrifugation (AUC), transmission electron microscopy (TEM), and scanning electron microscopy (SEM) as shown exemplarily in Fig. 1.

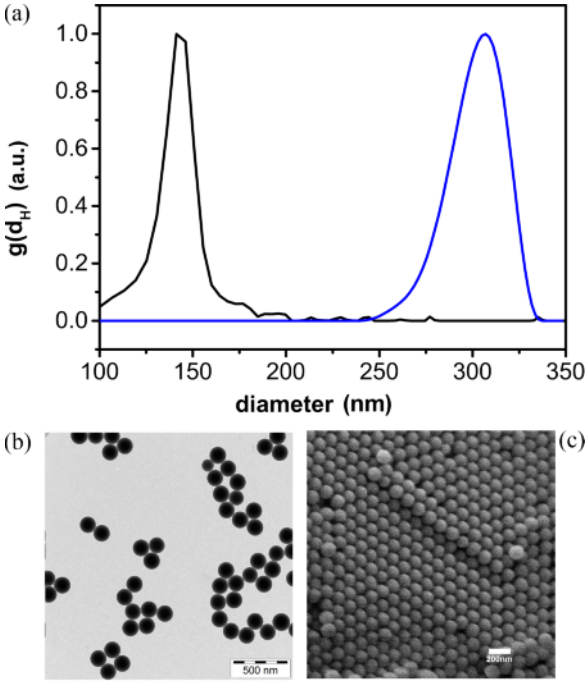

Fig. 1 (color online). Selected analytical data of the prepared PS spheres. (a) Particle size distribution functions determined by AUC; black ≅ sample with $d_{av} = 150$ nm, blue ≅ sample with $d_{av} = 300$ nm. TEM (b) and SEM (c) for the sample with $d_{av} = 150$ nm.

Centrifugation-induced crystallization of the mono-modal systems (reference system 1)

Before the systems containing two different particle sizes will be described, it is important to make sure that the application of a significant centrifugal force does not hamper the formation of colloidal crystals for the mono-modal dispersions as a reference state. First, a colloidal crystal was prepared *via* a conventional drying method; no centrifugation was applied. This sample was compared to materials prepared *via* centrifugation at fields varying up to 79 950 g (RCF). Monolithic colloidal crystals were obtained (see the photographic image shown in the Supporting Information

SI-1 available online; see note at the end of the paper for availability). In SEM one sees that at all conditions crystallization into close packing had occurred. However, the crystal domains are relatively small, and triangular defects occur frequently. Optical properties of the materials were investigated by UV/Vis reflectance measurements. The results of these measurements support our conclusion that the quality of the samples does not differ significantly if a centrifugal force is applied for ordering of the binary mixture. The position of the photonic stop-band ($\lambda_{SB} = 425$ nm; for $d_{PS} = 220$ nm) is not altered, which shows that there is no compression of the colloidal crystal due to the strong centrifugal force as a consequence of centrifugation. However, it can be seen that the width of the stop-band increases when the crystals are prepared with higher centrifugation speed. This indicates that the domain size is reduced, which is in agreement with the SEM images (see Supporting Information SI-1).

Crystallization of the binary system without application of centrifugal force (reference system 2)

A packing factor describing the ratio of the two PS sizes in a binary system is defined in the same manner as for atomic crystals:

$$Q_{PF} = \frac{d_{PS1}}{d_{PS2}} \tag{1}$$

with $d_{PS1} < d_{PS2}$. Considering the sphere sizes described above, Q_{PF} can vary between 0.433 and 0.916 for the binary systems in this study. Due to the similarity between the packing factor for the sodium chloride structure ($d(Na^+) = 2.04$ Å; $d(Cl^-) = 3.62$ Å; $Q_{PF} = 0.56$) we have selected the combination of $d_{PS1} = 154$ nm and $d_{PS2} = 300$ nm ($\Rightarrow Q_{PF} = 0.51$) for our study.

Before we investigated the influence of the centrifugation on the binary system, the following reference experiment was performed. A dispersion of the two PS sphere sizes was prepared by drying only with no centrifugation applied. The resulting solid material was characterized by SEM (Fig. 2). The sample consists of a mixture of large and small spheres. There is no phase separation between the two particle sizes. Significant parts of the sample are crystalline. The structure of the crystalline domains can be easily assigned to the NaCl structure (Fig. 2b). The lattice parameters of the bulk cell ($a_{bulk} = 428$ nm) and of the surface cell

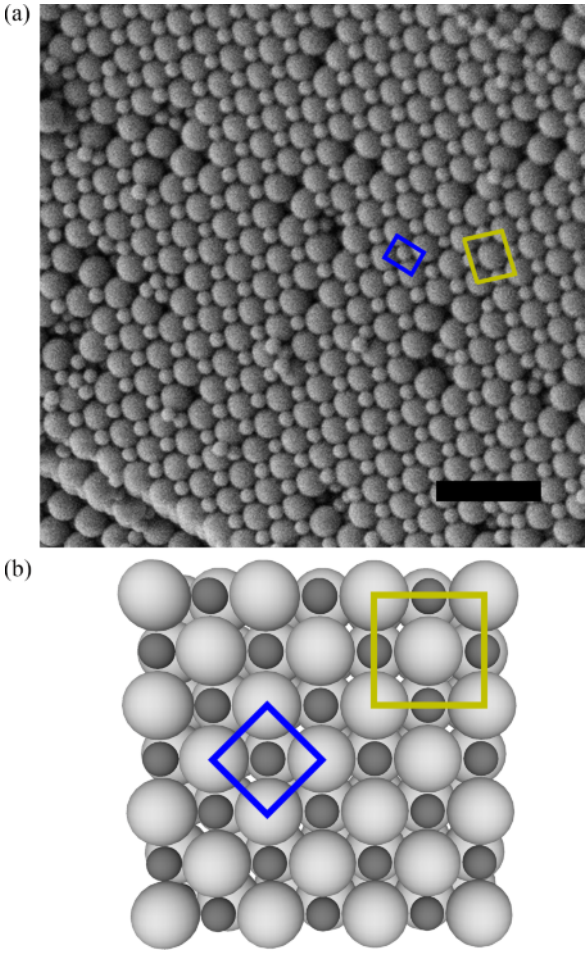

Fig. 2 (color online). (a) SEM image of the binary colloidal crystal obtained by drying only. PS spheres characterized by $Q_{PF} = 0.51$, $N_{PF} = 1$. Scale bar ≅ 1 μm. (b) View of the [100] lattice plane of NaCl structure. Bulk unit cell ≅ yellow; surface unit cell ≅ blue.

($a_{surf} = 301$ nm) fit very well to a close packing of the larger spheres PS2. The formation of the NaCl structure is not surprising since for the given Q_{PF} value it represents the thermodynamically most stable structure.

Structures obtained after preparative centrifugation of binary PS dispersions

The number of factors influencing the outcome of the sedimentation experiments is large. Not only the obvious parameter Q_{PF} is of importance, it has also been demonstrated that the absolute latex concentra-

tion is crucial since sedimentation coefficients are concentration dependent [66]:

$$N_{PF} = \frac{N_{PS1}}{N_{PS2}} \tag{2}$$

with $N_{PS1} \cong$ the initial number of the smaller PS spheres, and $N_{PS2} \cong$ the initial number of the larger PS spheres. Furthermore, the centrifugation speed and the centrifugation time determine the concentration gradients of each species and with it the locally varying concentrations of each of the species.

Therefore, Q_{PF} and N_{PF} were fixed, and the concentration dependence was investigated first.

We started with a concentration of 9 wt.-% 154 nm latex +21 wt.-% 300 nm latex ($Q_{PF} = 0.51$, $N_{PF} = 1$). Samples of the solid material obtained after centrifugation (76 min) and after drying taken from different positions along the direction of the centrifugal force field were investigated by SEM (Fig. 3). It can be seen that there is only a small region at the top where a higher fraction of the smaller spheres PS1 is present. At all other positions there is a homogeneous mixture of PS1 and PS2. However, unlike the crystalline domains seen in the reference system, only a glass-like state could be observed. Domains with long-range order could not be found. This is a first hint that the centrifugation-induced sedimentation and aggregation of the binary system (in contrast to the monodisperse system) does not necessarily lead to the thermodynamically controlled phases, but that kinetic factors play a major role. Therefore, next the latex concentrations were varied further keeping Q_{PF} and N_{PF} constant. The SEM micrographs taken from a sample prepared at 8 wt.-% 154 nm latex +19 wt.-% 300 nm latex (centrifugal time = 50 min) is shown in Fig. 4.

A clear separation effect can be deduced from the data. The top part of the sample is characterized by a majority of the smaller spheres PS1, and only few bigger spheres are present (Fig. 4a). The opposite is the case at the bottom positions (Fig. 4d). In between N_{PF} varies indicating a gradient formation with larger spheres enriching in the regions closer to the bottom of the centrifuge tube where a crystalline state (Fig. 4c) emerges. It is very difficult to deduce a crystal structure in 3D from SEM images which have mainly 2D character. Nonetheless, the structure seen in Fig. 3c resembles the aluminum boride AlB_2 structure with the following cell parameters: a ≈ 310 nm; c ≈ 430 nm. AlB_2

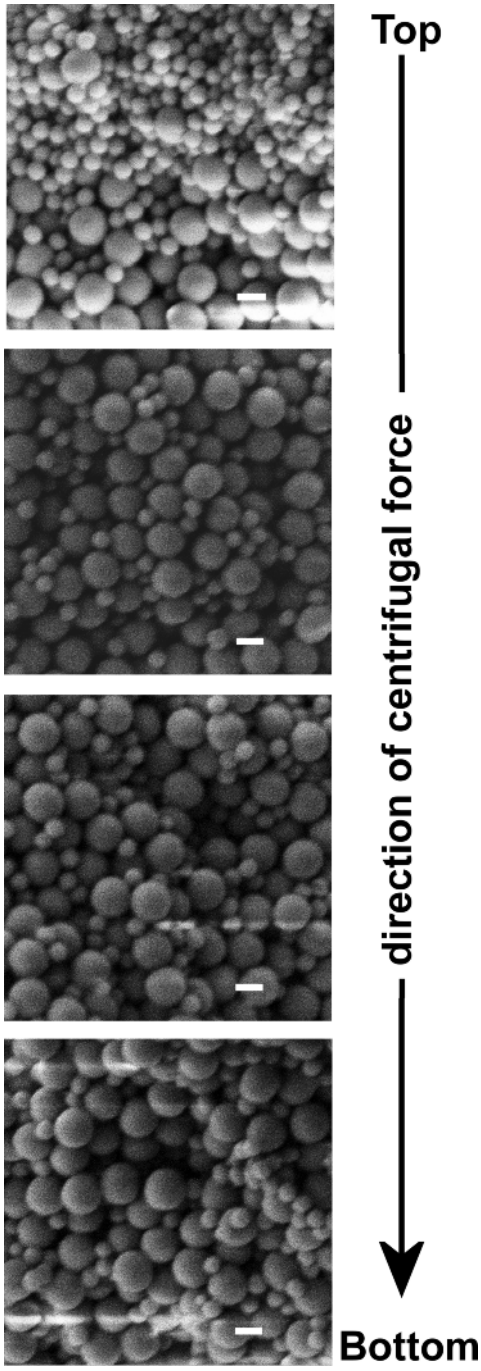

Fig. 3. Aggregation of binary PS systems of 154 nm (9 wt.-%) and 300 nm (21 wt.-%) latices ($Q_{PF} = 0.51$, $N_{PF} = 1$). The single SEM images (scale bars ≅ 200 nm) were recorded from samples taken at different positions along the direction of centrifugal force. TOP indicates the top of the vial used for centrifugation.

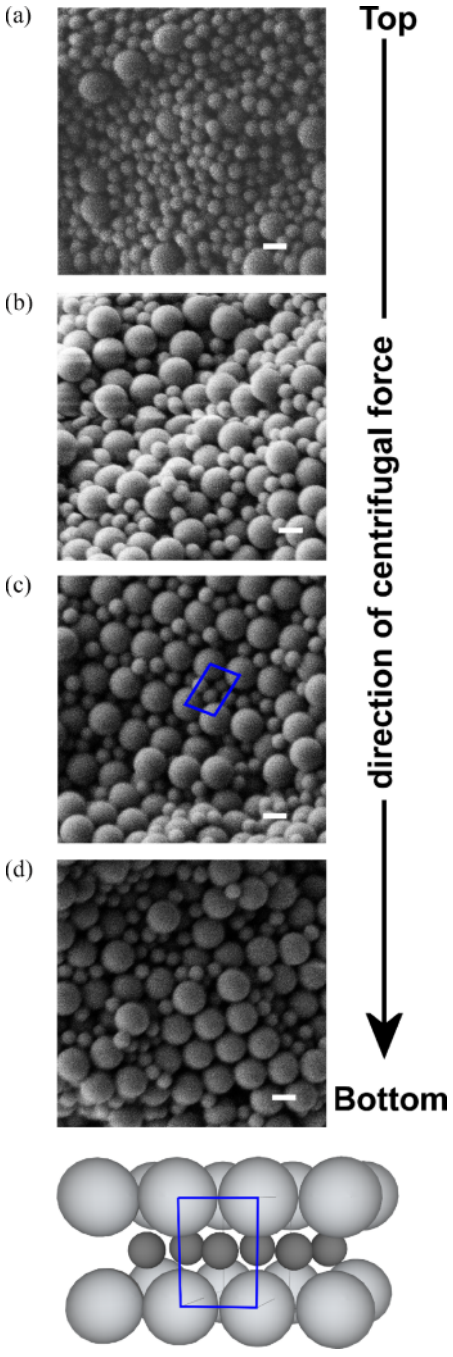

Fig. 4 (color online). Aggregation of binary PS systems of 154 nm (8 wt.-%) and 300 nm (19 wt.-%). The single SEM images (scalebars ≅ 200 nm) were recorded from samples taken at different positions along the direction of centrifugal force. TOP indicates the top of the vial used for centrifugation. In (c) the [100] face of the AlB_2 crystal structure is highlighted.

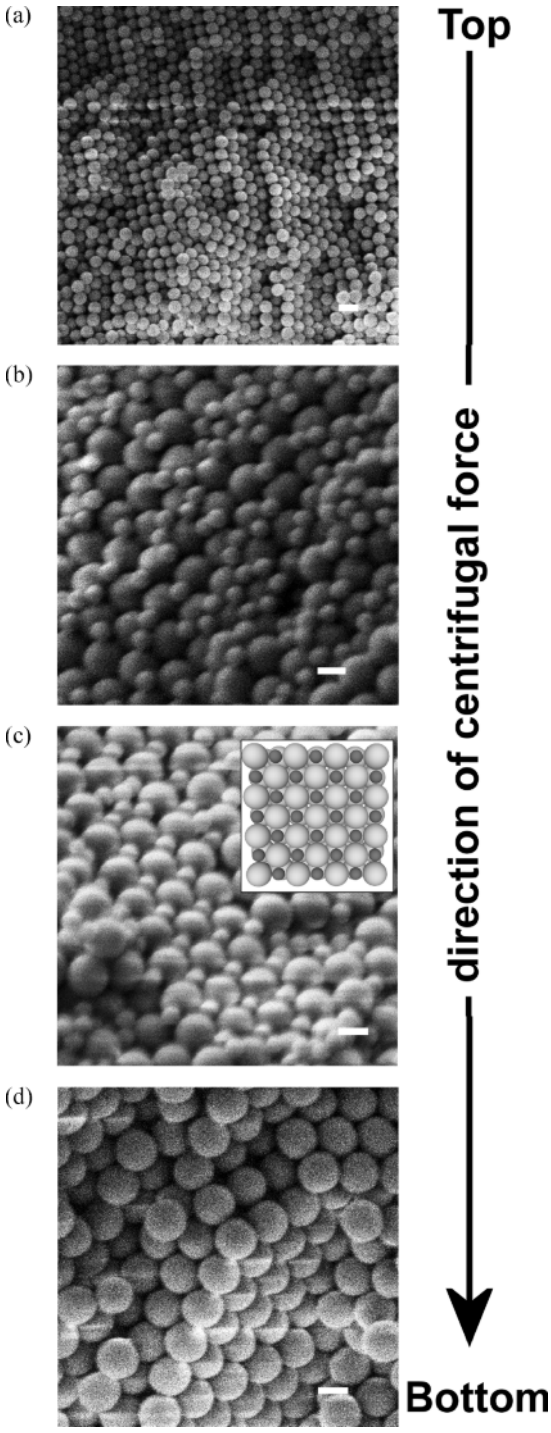

Fig. 5. Aggregation of binary PS systems of 154 nm (5 wt.-%) and 300 nm (12 wt.-%). The single SEM images (scalebars ≅ 200 nm) were recorded from samples taken at different positions along the direction of centrifugal force.

has hexagonal symmetry (space group P6/*mmm*). It comprises two densely packed layers of the larger spheres PS2 and one intercalated layer with PS1 in interstitial positions. It is obvious that the N_{PF} of the AlB_2 structure deviates from the initial N_{PF} value (= 1). The AlB_2 structure is an important structure for colloidal crystallization and has already been observed experimentally by others [34, 67, 68]. A further change of the latex concentrations to 5 wt.-% 154 nm latex +12 wt.-% 300 nm latex (centrifugal time = 28 min) leads to the situation shown in Fig. 5. The degree of order in the system has increased further, and as expected the separation of spheres with different size is more pronounced. One sees a distorted close packing of PS1 at the top (Fig. 5a) and at the bottom (Fig. 5d) a close packing of PS2. In between one can identify a crystalline binary phase corresponding to the NaCl structure (Fig. 5c).

Conclusion

In this study, we could demonstrate for the first time that centrifugation is a very promising technique to realize different packing structures in binary latex mixtures, even when their size and number ratio are kept constant. For the applied 154 nm and 300 nm latex mixture at equal number ratio, a NaCl structure was expected and found as the thermodynamically favored structure upon simple drying of the binary latex mixture. Investigating the same mixture in the centrifuge, the concentration of the latex adds an additional variable besides the experimental parameters for centrifugation. This leads to unordered structures as well as to the formation of the NaCl and AlB_2 structure together with unordered regions. Therefore, our study implies a great potential of centrifugation of binary and perhaps later on even ternary nanoparticle mixtures to form structural gradients including kinetically determined structures which can otherwise only rarely be obtained. The reason is the formation of individual concentration gradients for each of the species in the mixture leading to locally varying mixing ratios, which have varying driving forces towards different packing structures along the gradient.

Supporting information

Summarized analytical data for the centrifugation-induced crystallization of mono-modal dispersions of 220 nm PS spheres are given as Supporting Information available online (DOI: 10.5560/ZNB.2013-3001).

Acknowledgement

M. C. was funded by a Chinese Scholarship Council stipend.

[1] M. Jansen, *Angew. Chem. Int. Ed.* **2002**, *41*, 3746.
[2] P. Jiang, J. F. Bertone, K. S. Hwang, V. L. Colvin, *Chem. Mater.* **1999**, *11*, 2132.
[3] P. Jiang, J. F. Bertone, V. L. Colvin, *Science* **2001**, *291*, 453.
[4] Y. Yin, A. P. Alivisatos, *Nature* **2005**, *437*, 664.
[5] C. B. Murray, C. R. Kagan, M. G. Bawendi, *Annu. Rev. Mater. Sci.* **2000**, *30*, 545.
[6] Y. N. Xia, B. Gates, Y. D. Yin, Y. Lu, *Adv. Mater.* **2000**, *12*, 693.
[7] W. Stober, A. Fink, E. Bohn, *J. Colloid Interface Sci.* **1968**, *26*, 62.
[8] G. H. Bogush, M. A. Tracy, C. F. Zukoski, *J. Non-Cryst. Solids* **1988**, *104*, 95.
[9] A. Burneau, B. Humbert, *Colloids Surf. A* **1993**, *75*, 111.
[10] H. Giesche, *J. Eur. Ceram. Soc.* **1994**, *14*, 189.
[11] H. Giesche, *J. Eur. Ceram. Soc.* **1994**, *14*, 205.
[12] J. Park, J. Joo, S. G. Kwon, Y. Jang, T. Hyeon, *Angew. Chem. Int. Ed.* **2007**, *46*, 4630.
[13] F. X. Redl, K. S. Cho, C. B. Murray, S. O'Brien, *Nature* **2003**, *423*, 968.
[14] F. Candau, R. H. Ottewill, *An introduction to polymer colloids*, Kluwer, Dodrecht, **1990**.
[15] J. W. Goodwin, J. Hearn, C. C. Ho, R. H. Ottewill, *Colloid Polym. Sci.* **1974**, *252*, 464.
[16] C. M. Tseng, Y. Y. Lu, M. S. Elaasser, J. W. Vanderhoff, *J. Polym. Sci., Part A: Polym. Chem.* **1986**, *24*, 2995.
[17] C. E. Reese, C. D. Guerrero, J. M. Weissman, K. Lee, S. A. Asher, *J. Colloid Interf. Sci.* **2000**, *232*, 76.
[18] P. Pieranski, L. Strzelecki, B. Pansu, *Phys. Rev. Lett.* **1983**, *50*, 900.
[19] P. Pieranski, *Contemp. Phys.* **1983**, *24*, 25.
[20] B. T. Holland, C. F. Blanford, T. Do, A. Stein, *Chem. Mater.* **1999**, *11*, 795.
[21] S. Polarz, B. Smarsly, *J. Nanosci. Nanotechnol.* **2003**, *2*, 581.

[22] M. Trau, D. A. Saville, I. A. Aksay, *Langmuir* **1997**, *13*, 6375.
[23] M. Trau, D. A. Saville, I. A. Aksay, *Science* **1996**, *272*, 706.
[24] M. Holgado, F. Garcia-Santamaria, A. Blanco, M. Ibisate, A. Cintas, H. Miguez, C. J. Serna, C. Molpeceres, J. Requena, A. Mifsud, F. Meseguer, C. Lopez, *Langmuir* **1999**, *15*, 4701.
[25] N. D. Denkov, O. D. Velev, P. A. Kralchevsky, I. B. Ivanov, H. Yoshimura, K. Nagayama, *Nature* **1993**, *361*, 26.
[26] N. D. Denkov, O. D. Velev, P. A. Kralchevsky, I. B. Ivanov, H. Yoshimura, K. Nagayama, *Langmuir* **1992**, *8*, 3183.
[27] J. D. Joannopoulos, R. D. Meade, J. N. Winn, *Photonic Crystals*, Princeton University Press, Princeton, **1995**.
[28] J. D. Joannopoulos, P. R. Villeneuve, S. H. Fan, *Nature* **1997**, *386*, 143.
[29] E. Yablonovitch, *J. Opt. Soc. Am. B* **1993**, *10*, 283.
[30] D. Y. Wang, H. Möhwald, *J. Mater. Chem.* **2004**, *14*, 459.
[31] F. Li, D. P. Josephson, A. Stein, *Angew. Chem. Int. Ed.* **2011**, *50*, 360.
[32] S. Hachisu, S. Yoshimura, *Nature* **1980**, *283*, 188.
[33] P. Bartlett, R. H. Ottewill, P. N. Pusey, *Phys. Rev. Lett.* **1992**, *68*, 3801.
[34] N. Hunt, R. Jardine, P. Bartlett, *Phys. Rev. E: Stat. Phys., Plasmas, Fluids, Relat. Interdiscip. Top.* **2000**, *62*, 900.
[35] V. Kitaev, G. A. Ozin, *Adv. Mater.* **2003**, *15*, 75.
[36] L. Wang, Y. Wan, Y. Li, Z. Cai, H.-L. Li, X. S. Zhao, Q. Li, *Langmuir* **2009**, *25*, 6753.
[37] D. Y. Wang, H. Moehwald, *Adv. Mater.* **2004**, *16*, 244.
[38] Z. Zhou, Q. Yan, Q. Li, X. S. Zhao, *Langmuir* **2007**, *23*, 1473.
[39] F. Caruso, *Adv. Mater.* **2001**, *13*, 11.
[40] P. Bartlett, A. I. Campbell, *Phys. Rev. Lett.* **2005**, *95*.
[41] M. E. Leunissen, C. G. Christova, A. P. Hynninen, C. P. Royall, A. I. Campbell, A. Imhof, M. Dijkstra, R. van Roij, A. van Blaaderen, *Nature* **2005**, *437*, 235.
[42] M. E. Leunissen, H. R. Vutukuri, A. van Blaaderen, *Adv. Mater.* **2009**, *21*, 3116.
[43] M. D. Eldridge, P. A. Madden, D. Frenkel, *Nature* **1993**, *365*, 35.
[44] Y. G. Sun, Y. N. Xia, *Science* **2002**, *298*, 2176.
[45] T. Hyeon, *Chem. Commun.* **2003**, 927.
[46] J. Park, K. J. An, Y. S. Hwang, J. G. Park, H. J. Noh, J. Y. Kim, J. H. Park, N. M. Hwang, T. Hyeon, *Nat. Mater.* **2004**, *3*, 891.
[47] S. Polarz, *Adv. Funct. Mater.* **2011**, *21*, 3214.
[48] H. Cölfen, M. Antonietti, *Angew. Chem. Int. Ed.* **2005**, *44*, 5576.
[49] J. Fang, B. Ding, H. Gleiter, *Chem. Soc. Rev.* **2011**, *40*, 5347.
[50] M. Niederberger, H. Cölfen, *Phys. Chem. Chem. Phys.* **2006**, *8*, 3271.
[51] R.-Q. Song, H. Cölfen, *Adv. Mater.* **2010**, *22*, 1301.
[52] D. Schwahn, Y. Ma, H. Cölfen, *J. Phys. Chem. C* **2007**, *111*, 3224.
[53] C. Lausser, H. Cölfen, M. Antonietti, *ACS Nano* **2011**, *5*, 107.
[54] V. M. Yuwono, N. D. Burrows, J. A. Soltis, R. L. Penn, *J. Am. Chem. Soc.* **2010**, *132*, 2163.
[55] M. V. Kovalenko, M. Scheele, D. V. Talapin, *Science* **2009**, *324*, 1417.
[56] E. V. Shevchenko, D. V. Talapin, C. B. Murray, S. O'Brien, *J. Am. Chem. Soc.* **2006**, *128*, 3620.
[57] C. J. Kiely, J. Fink, M. Brust, D. Bethell, D. J. Schiffrin, *Nature* **1998**, *396*, 444.
[58] E. V. Shevchenko, D. V. Talapin, N. A. Kotov, S. O'Brien, C. B. Murray, *Nature* **2006**, *439*, 55.
[59] L. Filion, M. Dijkstra, *Phys. Rev. E: Stat., Nonlinear, Soft Matter Phys.* **2009**, *79*, 046714.
[60] M. J. Murray, J. V. Sanders, *Philos. Mag. A* **1980**, *42*, 721.
[61] J. V. Sanders, M. J. Murray, *Nature* **1978**, *275*, 201.
[62] A. Imhof, J. K. G. Dhont, *Phys. Rev. Lett.* **1995**, *75*, 1662.
[63] H. M. Strauss, E. Karabudak, S. Bhattacharyya, A. Kretzschmar, W. Wohlleben, H. Cölfen, *Colloid Polym. Sci.* **2008**, *286*, 121.
[64] S. K. Bhattacharyya, P. Maciejewska, L. Börger, M. Stadler, A. M. Gülsün, H. B. Cicek, H. Cölfen, *Prog. Colloid Polym. Sci.* **2006**, *131*, 9.
[65] H. Cölfen, T. M. Laue, W. Wohlleben, K. Schilling, E. Karabudak, B. W. Langhorst, E. Brookes, B. Dubbs, D. Zollars, M. Rocco, B. Demeler, *Eur. Biophys. J.* **2010**, *39*, 347.
[66] S. E. Harding, P. Johnson, *Biochem. J.* **1985**, *231*, 543.
[67] P. Bartlett, P. N. Pusey, *Physica A* **1993**, *194*, 415.
[68] D. K. Smith, B. Goodfellow, D. M. Smilgies, B. A. Korgel, *J. Am. Chem. Soc.* **2009**, *131*, 3281.